JOURNAL OF ELECTROMAGNETIC ENGINEERING AND SCIENCE, VOL. 17, NO. 2, 76~85, APR. 2017

http://dx.doi.org/10.5515/JKIEES.2017.17.2.76
ISSN 2234-8395 (Online) · ISSN 2234-8409 (Print)

Magnetic Resonant Wireless Power Transfer with Rearranged Configurations

Seok Hyon Kang · Chang Won Jung*

Abstract

We investigate the indirect-fed magnetic resonant wireless power transfer (MR-WPT) system for wireless charging for mobile devices by rearranging the loops and coils. Conventional MR-WPT is difficult to apply to consumer electronic products because of the arrangement of the resonators. In addition, there are restrictions for charging using a wireless technology, which depend on the circumstances of the usage scenarios. For practical applications, we analyzed the transfer efficiency of the MR-WPT system with various combinations and positions of resonators. Three rearranged configurations (*Out-Out*, *Out-In*, *In-In*) have been considered and experimentally investigated using hollow pipe loops and wire copper coils. There were four types of loops and two types of coils; each one had a different diameter and thickness. The results of the measurements show that the trends of the transfer efficiencies for the three configurations were similar. A transfer efficiency of 82.5% was achieved at a 35-cm distance between the 60-cm diameter transmitter (Tx) and receiver (Rx) coils.

Key Words: Indirect-Fed, Magnetic Resonant, Resonator, Wireless Power Transfer.

I. INTRODUCTION

After the successful demonstration of non-radiative wireless power transmission (WPT) by Professor Marin Soljacic's group at Massachusetts Institute of Technology in 2007, extensive research and standardization activities were carried out [1]. The conventional WPT, which uses the magnetic resonant coupling method, is difficult to apply to consumer electronic products. Several technical issues should be resolved to achieve a charging efficiency that is comparable with a wired charging apparatus. These issues include impedance matching, controlling the distance between the resonators, and aligning the resonators on the central axis. In addition, there are restrictions in terms of charging in a wireless technology, which depend on the circumstances of the usage scenarios. For the non-radiative strongly coupled magnetic resonance WPT (MR-WPT) discussed in [1], the charging can be done in the near-field range between the transmitting station and the receiving devices. The charging efficiency of the WPT can be determined by several elements, such as distance, alignments and angles of the coils and loops, matching circuits, and the physical parameters of the copper [2]. In fact, the alignments, arrangements, and angles of the coils and loops in the transmitting and receiving parts of the WPT can vary in practical circumstances. For example, to charge a mobile device, one may have to turn device either in an alternating direction or to a position that is opposite to the transmitting part for the electricity charging. These scenarios depend on the practical usage of the MR-WPT-embedded products. Thus, it seems essential to investigate the change in efficiency due to reconfiguring the positions of the coils and loops.

With regard to the efficiency of the MR-WPT, the material parameters of the coils and loops are also of significance. In [3],

Manuscript received November 15, 2016 ; Revised March 22, 2017 ; Accepted March 25, 2017. (ID No. 20161115-042J)
Graduate School of Nano·IT·Design Fusion, Seoul National University of Science and Technology, Seoul, Korea.
*Corresponding Author: Chang Won Jung (e-mail: changwoj@seoultech.ac.kr)

the influence of the physical parameters of copper on the charging efficiency was analyzed. To enhance the efficiency, the hollow pipe-based copper could be used for the coils and loops.

In this paper, we investigate the indirect-fed MR-WPT by rearranging the locations of the loops and coils using theoretical analysis, three-dimensional full wave simulation, and measurement analysis. The typical arrangement in the MR-WPT, source—transmitter (Tx) coil and receiver (Rx) coil—load, is limited for applications because the receiver part, which includes the Rx coil and load, would take up too much space in a mobile device or the Rx coil would be used as a repeater between the Tx part and mobile device with only load. Therefore, three rearranged configurations, *Out-Out*, *Out-In*, and *In-In*, have been considered for realistic applications. In general, the MR-WPT consists of circular resonators. We also study the effects of using various dimensions for the load, either a hollow pipe or thick copper wire, for each rearranged configuration.

This paper is organized as follows. The modeling and equivalent circuit theories are presented in Section II; simulated circuit parameters and the specifications of the coils and loops are also discussed. Section III shows the measurement results of the three kinds of rearranged MR-WPT configurations. An analysis of the measurement results follows in Section IV.

Ⅱ. Modeling of Rearranged MR-WPT

In general, the source and load loops are placed outside the Tx and Rx coils in a conventional MR-WPT. This configuration is well known and widely used. In this study, novel MR-WPT configurations are proposed as shown in Fig. 1. The distance between the Tx coil and the Rx coil is defined as the transfer distance (TD). Depending on the position of the source and load loops, the proposed MR-WPT are classified into three configurations. Fig. 1(a) shows the conventional system, which

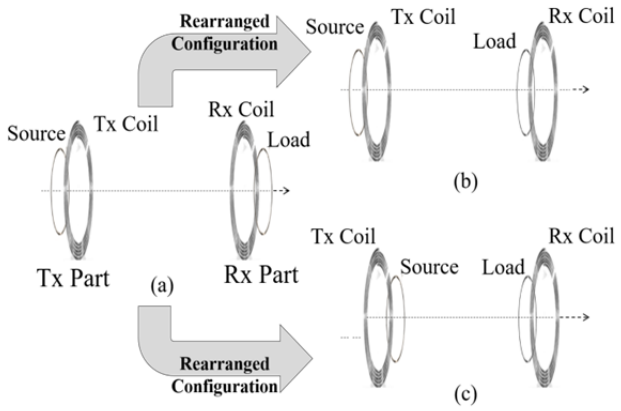

Fig. 1. Three rearranged magnetic resonant wireless power transfer (WPT) configurations. (a) *Out-Out* configuration, known as a conventional WPT, (b) *Out-In* configuration, and (c) *In-In* configuration.

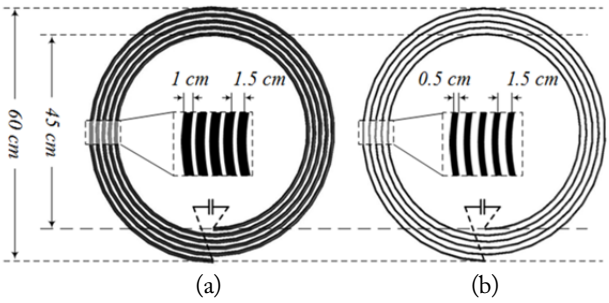

Fig. 2. The development of spiral coils for Tx and Rx resonators. (a) A spiral coil with pipe and (b) a spiral coil with wire.

we call the *Out-Out* configuration. In this configuration, the source and load loops are placed outside the Tx and Rx coils. One can also place either one or two loops inside the two resonant coils, which is called the *Out-In* and the *In-In* configurations as shown in Fig. 1(b) and (c), respectively.

1. Specifications of Coils and Loops

The strongly coupled MR-WPT is composed of two loops and two coils. The loops operate as the source and the load. Spiral coils are used for the Tx and Rx resonators. In this study, the spiral coils were made of copper pipes or copper wires. The copper pipe is hollow, and the diameter of the cross section of the pipe is 10 mm. The diameter of the cross section of the copper wire is 5 mm. Examples of fabricated spiral coils are shown in Fig. 2. One is made of a copper pipe and the other is made of copper wire. The diameter of each spiral coil is 60 cm. The pitch is 15 mm and the number of turns is 5.

We fabricated four types of loops with different dimensions as shown in Fig. 3 and Table 1. The diameters of the loops made of copper pipe are 20 cm, 30 cm, and 40 cm. A loop 40 cm in diameter was made of copper wire for comparison of performance in MR-WPT with a pipe loop of 40 cm in diameter. A pair of loops with the same diameter was constructed and used at the same time for the source and load.

2. Capacitance of Coils and Loops

All coils and loops were connected with capacitors to operate at the desired frequency. In the case of the spiral coils, the more

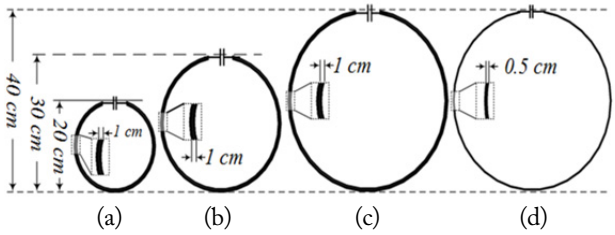

Fig. 3. Fabricated loops for the source and load. (a) Pipe loop 20 cm in diameter (b) pipe loop 30 cm in diameter, (c) pipe loop 40 cm in diameter, and (d) wire loop 40 cm in diameter.

Table 1. RLC and Q-factor of coils and loops

	Diameter(cm)	R (Ω)	L (nH)	C (nF)	Q factor
Pipe loop	20	0.02	386.45	-	147.20
	30	0.04	659.45	-	125.24
	40	0.07	955.33	-	89.59
Wire loop	40	0.07	1,123.88	-	112.06
Pipe coil	60	0.33	15,532.79	24.68	2,005.14
Wire coil	60	0.36	16,826.08	19.01	1,991.09

Table 2. Capacitance values connected to coils and loops

	Diameter (cm)	Simulated output value (pF)	Experimental value (pF)
Pipe loop	20	1,435.9	1,500.0
	30	835.6	820.0
	40	576.8	560.0
Wire loop	40	490.3	470.0
Pipe coil	60	10.0	6.0
Wire coil	60	13.0	10.0

windings, the higher the intrinsic capacitance obtained in the coils [4]. This is called self-capacitance. However, this self-capacitance value is so small as to be negligible [5]. Therefore, the coils and loops were connected with external capacitors in a series. Capacitors play important roles in achieving a resonant frequency at 6.78 MHz. This industrial, scientific, and medical (ISM) frequency has been declared to be the operating frequency band for the MR-WPT in the Alliance for Wireless Power (A4WP) version 1.0 baseline system specification [6]. For convenience, we numbered the resonators (loops and coils) in an arranged order (source loop, Tx coil, Rx coil, and load loop) from 1 to 4. The resonant frequency of the coils and loops can be expressed by the inductance and capacitance as follows:

$$f_0 = \frac{1}{2\pi\sqrt{L_i C_i}} \quad (\text{where } i = 1\text{-}4) \tag{1}$$

The capacitance C_i can be calculated using the desired resonant frequency and the inductance of the coils or loops. Each coil or loop can be simulated using the three-dimensional full-wave electromagnetic wave simulator (Ansoft HFSS version 12.0) to determine the inductance values. The capacitance is obtained using (1). The capacitor is connected to the coils or loops for matching resonant frequency. However, as shown in Table 2, the choice of the lumped capacitor shall be determined according to the commercial capacitor kits, because it approximated the value of a ready-made commercial capacitor. As shown in Table 1, there was a difference between the simulation results and the experimental values of resistance (R), inductance (L), capacitance (C), and quality factor (Q factor).

3. Equivalent Circuit of the Rearranged MR-WPT

The MR-WPT can be analyzed using two representative methods: the Z-matrix and the ABCD-matrix [7]. In this paper, the Z-matrix was used for the equivalent circuit analysis. Fig. 4 depicts the equivalent circuits for the three configurations of MR-WPT shown in Fig. 1. The coils and loops were represented by lumped R_i, L_i, and C_i (i=1–4), respectively. R_S and R_L (R_S=R_L=50 Ω) were input and output port impedances, respectively. Cross-coupling factor k values, such as k_{13}, k_{14}, and k_{24}, were neglected for simplicity [8, 9].

In realizing the system, the Tx and Rx are kept symmetrical

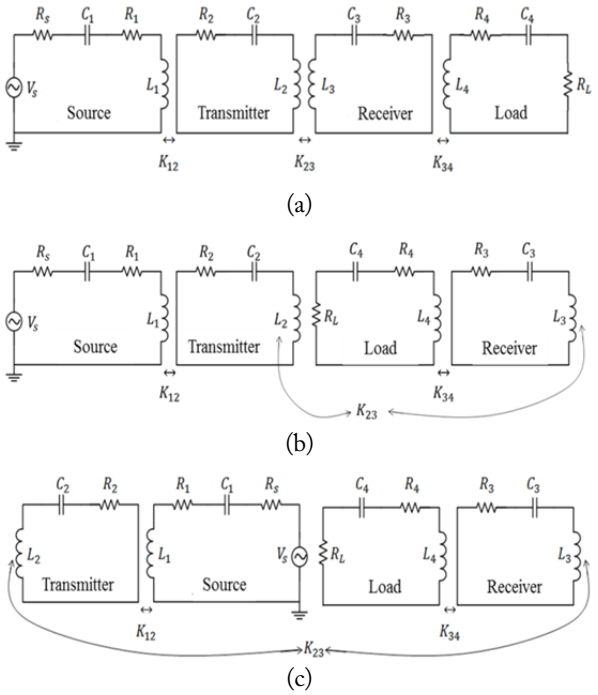

Fig. 4. Equivalent circuits of rearranged magnetic resonant wireless power transfer systems. (a) *Out-Out* conventional system, (b) *Out-In* configuration, and (c) *In-In* configuration.

and, thus, $R_S + Z_1 = R_L + Z_4$, and $R_2 = R_3$. The transmitter part has a source loop and a Tx coil. Likewise, the receiver part has a load loop and an Rx coil. This is explained in the following section. The equivalent circuit of Fig. 4(a) is expressed by the KVL matrix.

$$\begin{bmatrix} I_1 \\ I_2 \\ I_3 \\ I_4 \end{bmatrix} = \begin{bmatrix} R_S + R_1 & j\omega M_{12} & 0 & 0 \\ j\omega M_{12} & R_2 & j\omega M_{23} & 0 \\ 0 & j\omega M_{23} & R_3 & j\omega M_{34} \\ 0 & 0 & j\omega M_{34} & R_L + R_4 \end{bmatrix}^{-1} \begin{bmatrix} V_s \\ 0 \\ 0 \\ 0 \end{bmatrix} \quad (2)$$

To obtain the transfer efficiency (TE), we shall use the alternating currents of the source and load loops. Therefore, we can solve the KVL matrix using the substitution method to obtain I_1 and I_4 as follows:

$$I_1 = \frac{V_S}{\det A}\{R_{coil}{}^2 R_{loop} - R_{coil}(j\omega M_{34})^2 - R_{loop}{}^2 (j\omega M_{23})^2\}$$
$$I_4 = \frac{V_S}{\det A}\{-(j\omega M_{12})(j\omega M_{23})(j\omega M_{34})\} \quad (3)$$

M_{ij} is the mutual inductance that is generated between the i^{th} and j^{th} loops or coils. It can be calculated as:

$$M_{ij} = k_{ij}\sqrt{L_i L_j} \ (i = 1\text{–}3, \quad j = i + 1, 0 \le k_{ij} \le 1). \quad (4)$$

Mutual inductances happen on all occasions, such as M_{13}, M_{14}, and M_{24}. As stated above, it was assumed that the cross-coupling factor k values, such as k_{13}, k_{14}, and k_{24}, were 0. Therefore, the mutual inductance, M, was 0.

The Q factor, is another critical parameter with the coupling factor k. The higher the Q factor and coupling factor k, the greater the TE of the MR-WPT and the greater the TD [2]. In this symmetric system, paired coils and loops were used. This means that the source loop and the load loop have the same Q factor. The same is true for the coils. The Q factor can be obtained from:

$$Q_{loop} = \frac{\omega L_{loop}}{R_i + R_k} \ (i = 1, 4 \ \& \ k = S, L) \qquad Q_{coil} = \frac{\omega L_{coil}}{R_{coil}} \quad (5)$$

Using (3), mutual inductance (4), and Q factor (5), it is possible to express the ratio of input and output voltage as:

$$\frac{V_L}{V_S} = \frac{I_4(R_4 + R_L)}{I_1(R_1 + R_S)} = \frac{-(j\omega M_{12})(j\omega M_{23})(j\omega M_{34})}{R_{coil}{}^2 R_{loop} - R_{coil}(j\omega M_{34})^2 - R_{loop}{}^2 (j\omega M_{23})^2}$$
$$= \frac{jk_{12}k_{23}k_{34}Q_{loop}Q_{coil}{}^2 R_{loop}R_{coil}{}^2}{R_{coil}{}^2 R_{loop} + \omega k_{34}R_{coil}\sqrt{Q_{coil}Q_{loop}}\sqrt{R_{coil}R_{loop}} + \omega k_{23}R_{loop}{}^2 Q_{coil}R_{coil}} \quad (6)$$

Finally, the equation between η and S_{21} was derived from the (6) for the TE of the MR-WPT [10].

$$\eta = \frac{P_{out}}{P_{in}} = \frac{V_L{}^2/(R_4 + R_L)}{V_S{}^2/\{4(R_1 + R_S)\}} = |S_{21}|^2 \quad (7)$$

Using the Eq. (7) and the *RLC* values in Table 1, the calculated TE values for the four cases of MR-WPT with Tx and Rx pipe coils were obtained as shown in Fig. 5. The TE values were plotted according to the coupling factor between the Tx and Rx pipe coils. For a high coupling factor, the TE of a system with relatively large resonators for the source and load was high. Conversely, for a low k, the TE of a MR-WPT with relatively small loop as source and load was relatively low.

By measuring the S_{21} measured by the network analyzer, one can calculate the TE for the MR-WPT using Eq. (7). Note that the analysis of the *Out-In* and *In-In* systems can be carried out in the same manner as described above. It can be determined that the results of *Out-In* and *In-In* configurations will be the same as for the *Out-Out* configuration. Both have the same equation sets to describe them. Therefore, the three configurations of the MR-WPT can be simulated using the same analytical equations.

Ⅲ. Measurement of Rearranged MR-WPT

This section shows the detailed measurement method Used to determine the TEs of the rearranged MR-WPT systems. Previous studies have reported on the analysis of the results of efficiencies [11]. In these previous works, for the measurements of the TEs for various distances, the locations of both the source and load loops were simultaneously controlled by changing the gap between the loop and coil. And the gaps between the loop and coil in Rx and Tx parts are same [2, 12, 13]. In this study, the source loop was 6 cm from the Tx coil in all three configurations (*Out-Out, Out-In,* and *In-In*). Only the load loop was moved back and forth from the Rx coil to determine the optimal coupling factor k. Note that the highest S_{21} and the lowest S_{11} can be observed when the impedance matching condition is achieved with the optimum coupling factor k.

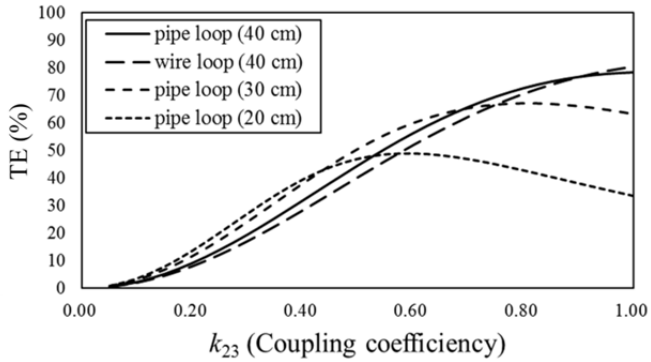

Fig. 5. The calculated TE of MR-WPT with Tx and Rx coils according to the coupling factor.

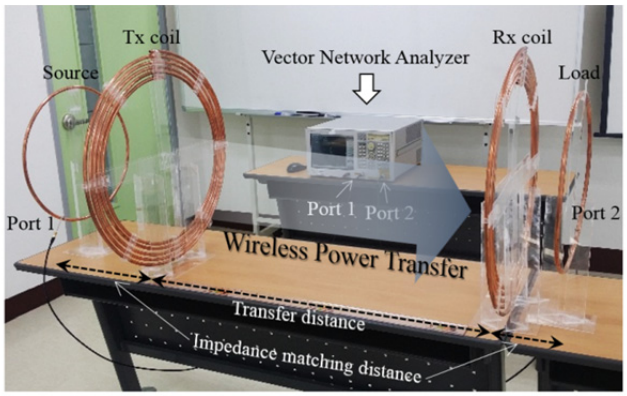

Fig. 6. The measurements of magnetic resonant wireless power transfer system. The locations of the coils are fixed, while that of the loops is changed, such as *Out* or *In* location of source and load.

Table 3. The list of measured rearranged configurations

Rearranged configuration	Coil	Source and load (diameter size)
Out-Out	Pipe	Pipe loop (D = 20, 30, 40 cm)
		Wire loop (D = 40 cm)
	Wire	Pipe loop (D = 20, 30, 40 cm)
		Wire loop (D = 40 cm)
Out-In	Pipe	Pipe loop (D = 20, 30, 40 cm)
		Wire loop (D = 40 cm)
	Wire	Pipe loop (D = 20, 30, 40 cm)
		Wire loop (D = 40 cm)
In-In	Pipe	Pipe loop (D = 20, 30, 40 cm)
		Wire loop (D = 40 cm)
	Wire	Pipe loop (D = 20, 30, 40 cm)
		Wire loop (D = 40 cm)

As discussed in Section II–1, two types of coils and four types of loops were used (Fig. 6). Each measurement was carried out by changing the TD from 15 cm to 100 cm in steps of 5 cm. At each distance, the gap between the Rx coil and the load loop was optimized to get the highest S_{21} response. An Agilent vector network analyzer (E5071B) was used to measure the *S*-parameters. The input power level and impedance were set to 1 mW (0 dBm) and 50 Ω, respectively.

The optimization was conducted by symmetrically changing the distance between the loop and coil for a high TE. Even though the TDs are same, the reflection coefficiency, S_{11}, is different according to the distance between the loop and coil. We marked the highest TE at each TD through optimization.

For the purpose of TE comparisons, we defined a measurement frequency for each configuration. When the TD was 100 cm, we measured the resonance frequency (f_{100cm}) and S_{21}. For the *In-In* case, S_{21} was measured up to 30 cm because there was not enough space between the coils due to the location of the loops. Therefore, at f_{100cm}, the S_{21} was measured. At a given distance, the maximum S_{21} value and the corresponding frequency were also measured. For analysis of the three different configurations, S_{21} (dB) was converted to η (%) using Eq. (7). Table 3 summarizes the experiments we carried out. For each configuration, eight different combinations of coils and loops were considered. Experiments for measuring the TE were executed sequentially according to Table 3.

Ⅳ. Analysis of Measurement Results

This section describes the measurement results of MR-WPT. The resonant frequencies for the pipe coils and wire coils when the TD was 100 cm were 6.92 ± 0.003 MHz and 7.03 ± 0.004 MHz, respectively. There was a slight difference in resonance frequencies (110 kHz) depending on the material used for the coil. We found that the actual inductance of the pipe coil was slightly larger than that of the wire coil, even though they were intended to be the same. Also, it is acknowledged that variations of these frequencies for either the pipe or wire coil were negligibly small, 3–4 kHz, regardless of the diameter of the loop. Because the system operates with magnetic resonance, the resonance frequency remained almost the same irrespective of loop size.

Table 4 shows the measured TE for the given frequency (f_{100cm}) for all the experiment combinations. There was a significant difference in the TE for the two different types of coils. The TE values for the pipe coils were typically higher than for the wire coils because of the skin effect and the surface of the structure. The surface has an effect on the current of the coils that gener-

Table 4. The transfer distance (TE) and the transfer efficiency (TD) between two coils of the MR-WPT at f_{100cm}

	Loop (diameter size)	*In-In*		*Out-In*		*Out-Out*	
		TE (%)	TD (cm)	TE (%)	TD (cm)	TE (%)	TD (cm)
Pipe coil	Pipe loop (D = 20 cm)	30.94	95	34.72	100	33.03	95
	Pipe loop (D = 30 cm)	67.87	65	71.60	60	68.20	65
	Pipe loop (D = 40 cm)	76.51	45	80.33	35	77.87	40
	Wire loop (D = 40 cm)	77.74	40	77.88	40	74.30	35
Wire coil	Pipe loop (D = 20 cm)	21.48	80	21.41	80	23.97	80
	Pipe loop (D = 30 cm)	64.31	65	64.03	65	63.95	65
	Pipe loop (D = 40 cm)	75.53	45	82.57	35	74.20	45

ate the magnetic field. To effectively analyze the measurement results, the three rearranged configurations, the types of coils and loops used, and the resonant frequency were investigated. The details are discussed in the following sections.

1. Comparisons of MR-WPT for Different Rearrangements

The TE for each TD was measured at f_{100cm}. Fig. 7 shows the comparison results of the TEs for the three configurations (*Out-Out, Out-In,* and *In-In*) for different diameters and types of loops. Figs. 8 and 9 show the trends in TE according to the loop resonators in the MR-WPT systems using pipe coils and wire coils. Regardless of the configuration types, the efficiencies were almost the same.

From these experiments, it was found that changing the positions of the source and load loops had little effect on the MR-WPT. A slight difference among the three configurations occurred due to the cross-coupling factor k, such as k_{13}, k_{24}, and k_{14}, which were not included in this study. When the wire coils were used as the Tx and Rx, the analysis produced the same conclusions as shown in Figs. 7–9.

2. Comparisons of Performance of MR-WPT for Different Coils and Loops

Fig. 7 displays the TE versus TD for different types of coils and loops. Based on these measurement results, we recognize that the larger the diameter of the loops, the higher the TE of the MR-WPT irrespective of the type of coils used in the system. However, as the TD increases, the TE decreases. In addition, the trends in TE according to the thickness of the cross-section of the resonators are almost the same.

$$\delta = \sqrt{\frac{\rho}{\pi \times f_0 \times \mu}} \tag{8}$$

According to Eq. (8), the skin depth is 0.65 μm at 6.78 MHz, where the resistivity (ρ) is 1.678×10^{-6} Ω·cm and the absolute magnetic permeability (μ) is $4\pi \times 10^{-7}$ H/m. If the skin depth at the resonant frequency, 6.78 MHz, is enough (Fig. 10), the radius of the resonator is the critical dimension that affects the performance of the MR-WPT. We obtained the same results as previous studies [9]. It was a common phenomenon with either pipe or wire coils in the Tx and Rx.

3. TE of the MR-WPT with Respect to the Resonant Frequency

As the TD decreases, the splitting of the resonant frequency occurs because of mutual inductance M_{23} between the two coils. The two resonances are odd mode and even mode [2]. Resonant frequencies of odd mode and even mode are expressed as f_{odd} and f_{even}, respectively, as follows:

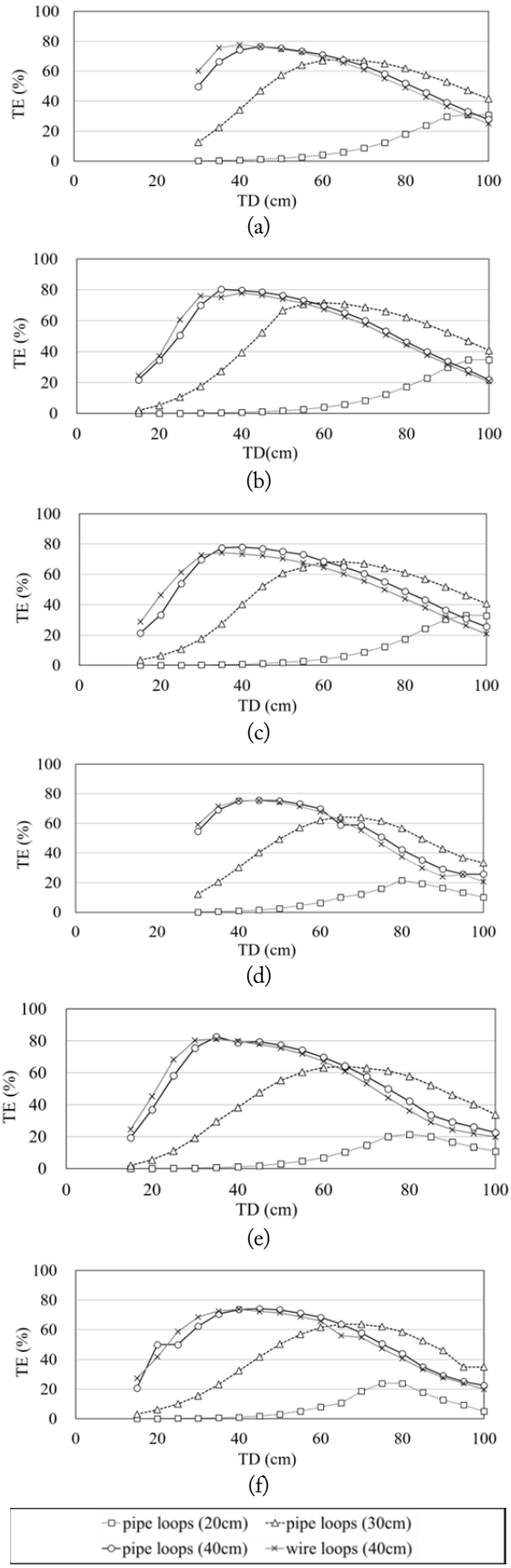

Fig. 7. The transfer efficiency (TE) according to the types of loops used as source and load. (a) *In-In* with pipe coils, (b) *Out-In* with pipe coils, (c) *Out-Out* with pipe coils, (d) *In-In* with wire coils, (e) *Out-In* with wire coils, and (f) *Out-Out* with wire coils.

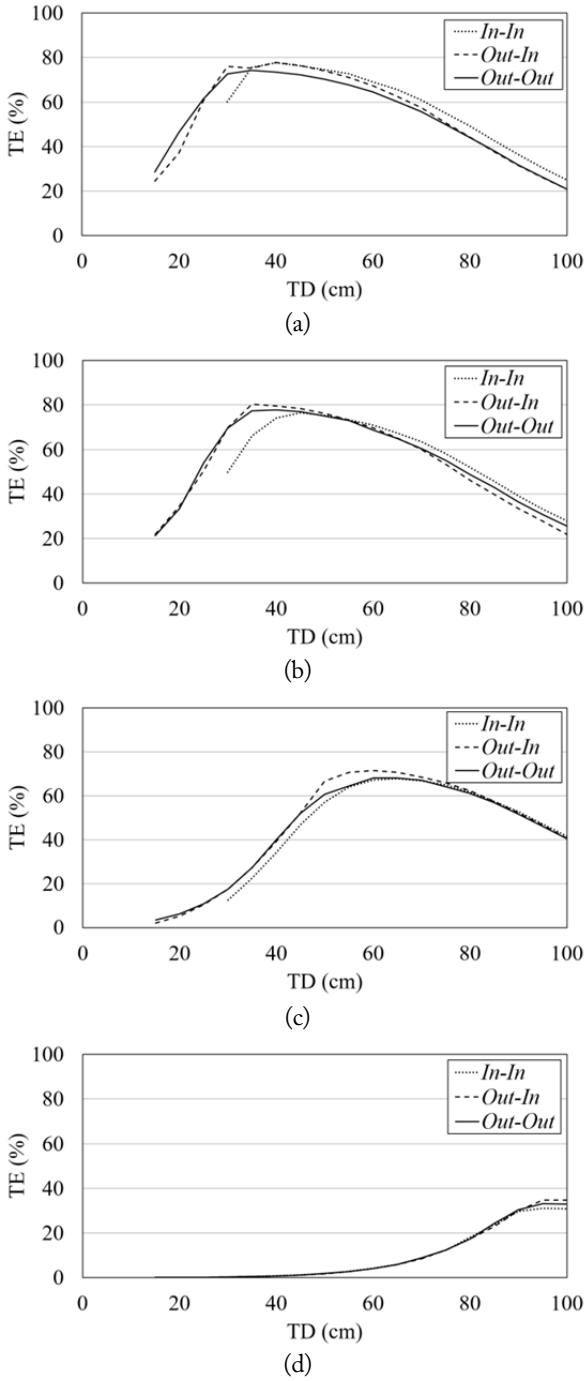

Fig. 8. The trends in transfer efficiency (TE) according to the loop resonators in magnetic resonant wireless power transfer system using pipe coils. (a) Wire loops 40 cm, (b) pipe loops 40 cm, (c) pipe loops 30 cm, and (d) pipe loops 20 cm.

$$f_{odd} = \frac{1}{2\pi\sqrt{(L_{2,3} + M_{23})C_{2,3}}} \tag{9}$$

$$f_{even} = \frac{1}{2\pi\sqrt{(L_{2,3} - M_{23})C_{2,3}}} \tag{10}$$

As the TD decreases, the M_{23} increases. There are two peaks of S_{21} for the left (f_{odd}) and right (f_{even}) around f_{100cm}. According to the measurement results, the highest S_{21} appeared at f_{even} rather than at f_{100cm} [2].

With regards to the TE, there were two aspects to consider. One was the S_{21} at f_{100cm}, and the other was the highest S_{21} at f_{even}. So far, the TE mentioned was the value η ($|S_{21}|^2$) at f_{100cm}. In this section, we made a comparison between f_{100cm} and f_{even}.

Fig. 11 depicts the measurement results of the TE for the *Out-Out* configuration at the two frequencies. It compares the TE at f_{100cm} with the highest TE at the same TD. The results for

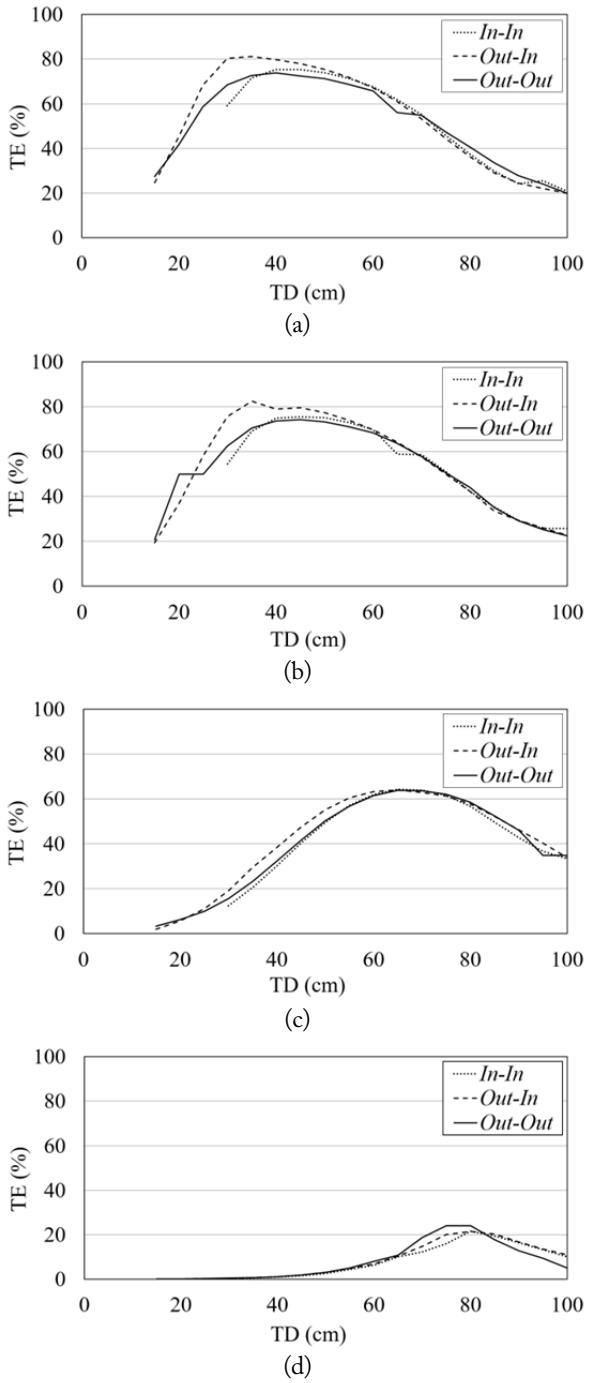

Fig. 9. The trends in transfer efficiency (TE) according to the loop resonators in magnetic resonant wireless power transfer system using wire coils. (a) Wire loops 40 cm, (b) pipe loops 40 cm, (c) pipe loops 30 cm, and (d) pipe loops 20 cm.

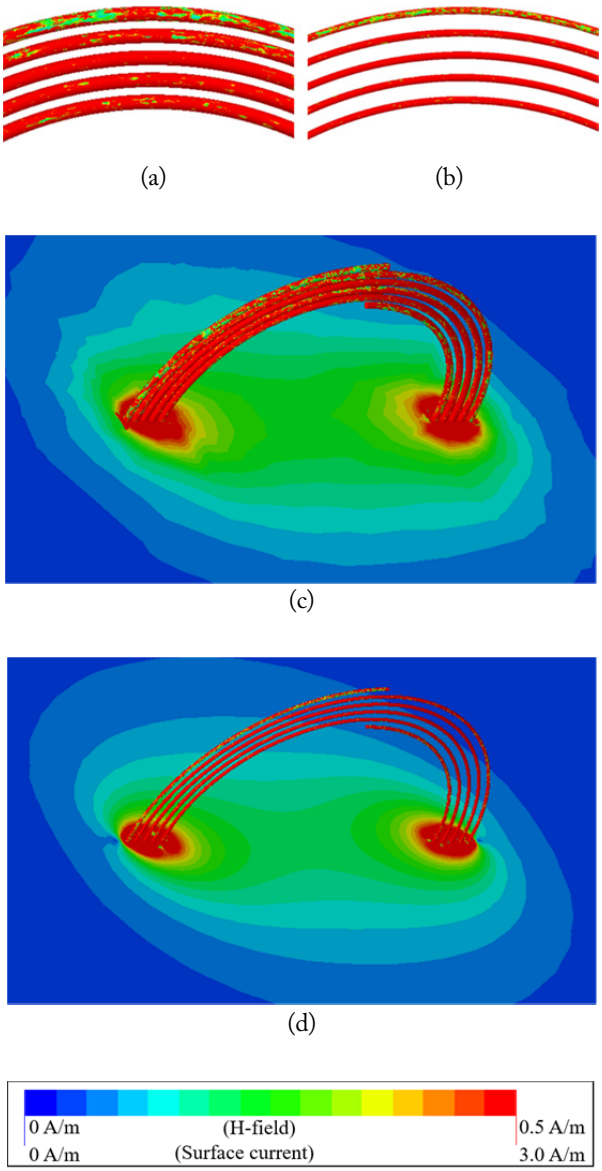

Fig. 10. The distributions of surface current and H-field of the spiral coil. (a) Surface current of a spiral coil with a 10 mm thickness, (b) surface current of a spiral coil with a 5 mm thickness, (c) spiral coil with a 10 mm thickness, and (d) spiral coil with a 5 mm thickness.

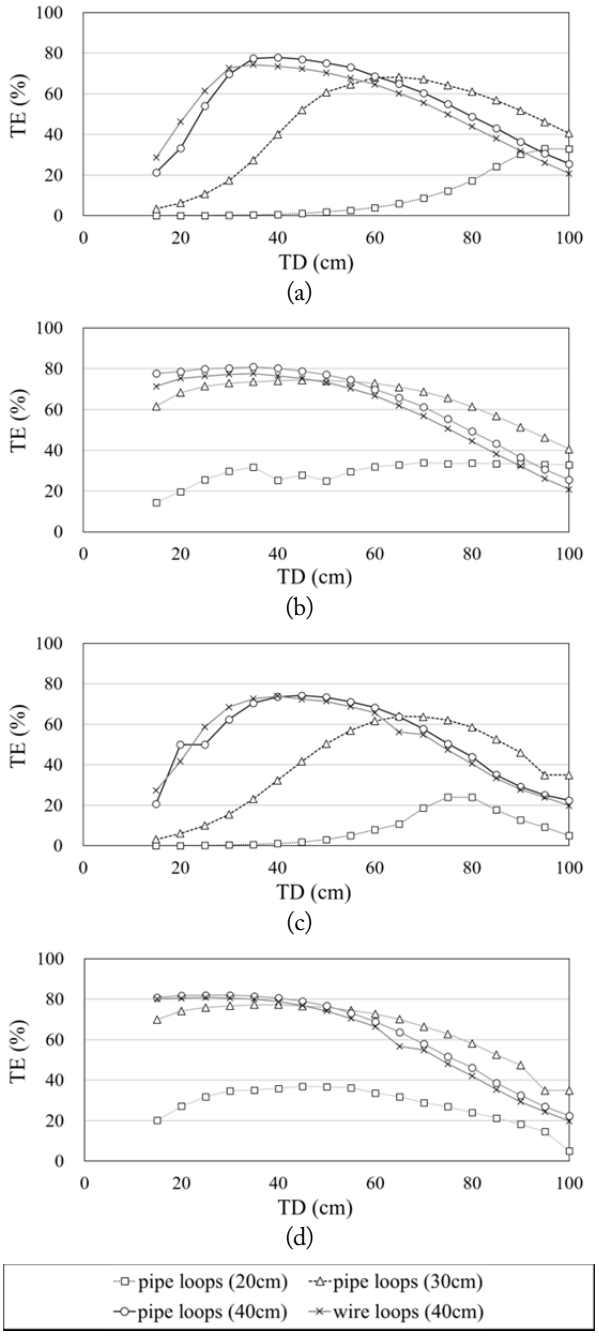

Fig. 11. The comparison between the transfer efficiency (TE) at f_{100cm} and the highest TE at the same transfer distance (TD). (a) The TE of pipe coils at f_{100cm}, (b) the highest TE of pipe coils, (c) the TE of wire coils at f_{100cm}, and (d) the highest TE of wire coils.

systems with pipe coils are shown in Fig. 11(a) and (b), while the results for systems with wire coils are given in Fig. 11(c) and (d). The trend of TE at f_{100cm} in Fig. 11(a) and (c) show a rapid decrease as the two coils come closer to each other. Conversely, the highest efficiencies for the pipe and wire coils remain relatively constant compared with the region of falling edge in Fig. 11(a) and (c).

The frequencies for the highest S_{21} for different TDs are measured and illustrated in Fig. 12. In the case of the system with pipe coils, the resonant frequency changed from 6.92 MHz to 8.09 MHz and from 7.03 MHz to 8.14 MHz for the system with the wire coils as the TD decreased. When the TD was decreased from 100 cm to about 40 cm, the resonant frequency in the two systems with wire coils and pipe coils changed 0.120 MHz and 0.114 MHz, respectively. This means that the frequency for the highest TE is almost constant and reaches f_{100cm} unless the TD goes below 40 cm. However, below 40 cm, the fractional change in the frequency for the highest TE increases to 90%.

According to the measurement results, when the TD increases, the frequency for the highest TE converges to average f_{100cm}

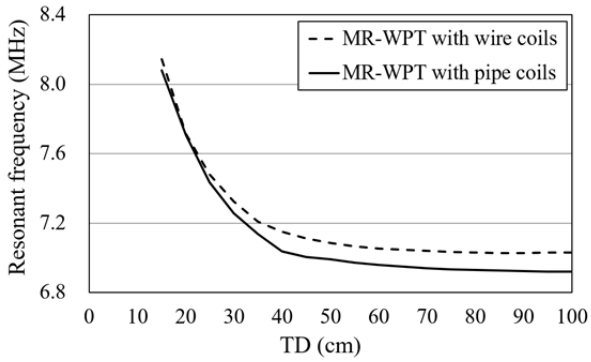

Fig. 12. The change in resonant frequency as transfer distance (TD) decreases. The results were divided into two groups according to the types of coils used.

values.

V. CONCLUSION

In this paper, we investigate feasible MR-WPT configurations, such as *Out-Out, Out-In*, and *In-In*, with respect to analytical theories, different coils and loops, their combinations, and their resonance frequencies. When the three configurations were compared, the power efficiencies are almost the same. This means that the position of the resonator has less impact on the TE of the MR-WPT system. This result came up with solutions for applications to wireless charging of mobile devices at the space restriction using proposed MR-WPT with rearranging resonators. This study can contribute to a wide variety of wireless charging applications for mobile devices.

This work was supported by the National Research Foundation of Korea Grant funded by the Korean Government (No. 2016R1D1A1B02012957).

REFERENCES

[1] A. Kurs, A. Karalis, R. Moffatt, and J. D. Joannopoulos, P. Fisher, and M. Soljacic, "Wireless power transfer via strongly coupled magnetic resonances," *Science*, vol. 317, no. 5834, pp. 83–86, 2007.

[2] A. P. Sample, D. T. Meyer, and J. R. Smith, "Analysis, experimental results, and range adaptation of magnetically coupled resonators for wireless power transfer," *IEEE Transactions on Industrial Electronics*, vol. 58, no. 2, pp. 544–554, 2011.

[3] H. C. Son, J. W. Kim, Y. J. Park, and K. H. Kim, "Efficiency analysis and optimal design of a circular loop resonance coil for wireless power transfer," in *Proceedings of Asia-Pacific Microwave Conference*, Yokohama, Japan, 2010, pp. 849–852.

[4] G. Grandi, M. Kazimierczuk, A. Massarini, and U. Reggiani, "Stray capacitances of single-layer air-core inductors for high-frequency applications," in *Conference Record of the 1996 IEEE Industry Applications Conference*, San Diego, CA, 1996, pp. 1384–1388.

[5] B. H. Waters, B. J. Mahoney, G. Lee, and J. R. Smith, "Optimal coil size ratios for wireless power transfer applications," in *Proceedings of 2014 IEEE International Symposium on Circuits and Systems (ISCAS)*, Melbourne, Australia, 2014, pp. 2045–2048.

[6] R. Tseng, B. von Novak, S. Shevde, and K. A. Grajski, "Introduction to the alliance for wireless power loosely-coupled wireless power transfer system specification version 1.0," in *Proceedings of 2013 IEEE Wireless Power Transfer (WPT)*, Perugia, Italy, 2013, pp. 79–83.

[7] J. H. Kim, B. C. Park, and J. H. Lee, "New analysis method for wireless power transfer system with multiple n resonators," *Journal of Electromagnetic Engineering and Science*, vol. 13, no. 3, pp. 173–177, 2013.

[8] Y. Zhang, Z. Zhao, and K. Chen, "Frequency splitting analysis of magnetically-coupled resonant wireless power transfer," in *Proceedings of 2013 IEEE Energy Conversion Congress and Exposition (ECCE)*, Denver, CO, 2013, pp. 2227–2232.

[9] H. Hwang, J. Moon, B. Lee, C. H. Jeong, and S. W. Kim, "An analysis of magnetic resonance coupling effects on wireless power transfer by coil inductance and placement," *IEEE Transactions on Consumer Electronics*, vol. 60, no. 2, pp. 203–209, 2014.

[10] R. K. Mongia, I. J. Bahl, and P. Bhartia, *RF and Microwave Coupled-Line Circuit*. Norwood, MA: Artech House, 2007.

[11] H. Hoang, S. Lee, Y. Kim, Y. Choi, and F. Bien, "An adaptive technique to improve wireless power transfer for consumer electronics," *IEEE Transactions on Consumer Electronics*, vol. 58, no. 2, pp. 327–332, 2012.

[12] T. P. Duong and J. W. Lee, "Experimental results of high-efficiency resonant coupling wireless power transfer using a variable coupling method," *IEEE Microwave and Wireless Components Letters*, vol. 21, no. 8, pp. 442–444, 2011.

[13] J. Kim, W. S. Choi, and J. Jeong, "Loop switching technique for wireless power transfer using magnetic resonance coupling," *Progress In Electromagnetics Research*, vol. 138, pp. 197–209, 2013.

Seok Hyon Kang

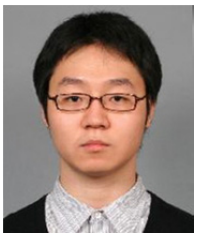

received his B.S. and M.S. degrees in Optometry from Seoul National University of Science and Technology (SeoulTech), Seoul, Korea, in 2010 and 2014, respectively. He is currently working toward Ph.D. degree in Electrical Engineering from Seoul National University of Science and Technology (SeoulTech), Seoul, Korea. His current research interest focuses on wireless power transfer.

Chang Won Jung

received his B.S. degree in Radio Science and Engineering from Kwang Woon University, Korea, in 1997, his M.S. degree in Electrical Engineering from the University of Southern California, Los Angeles, U.S., in 2001, and his Ph.D in Electrical Engineering and Computer Science from the University of California, Irvine, USA, in 2005. Since 2008, he has been an assistant professor with the Graduate School of Nano · IT · Design Fusion, Seoul National University of Science and Technology. From 1997 to 1999, he was a research engineer in the wireless communication department of LG Information and Telecommunication in Korea. From 2005 to 2008, he was a senior research engineer in the communication laboratory of Samsung Advanced Institute of Technology, Korea. He has published a book, over 110 papers in refereed journals and conference proceedings, and more than 40 international patents. He was the recipient of the International Telemetering Conference 2005 Best Paper Award and the ISAP 2010 Best Paper Award. His current research interests are antennas for MMMB communication systems, multifunctional reconfigurable antennas, EMI/EMC, millimeter-wave applications, and wireless power transfer for energy harvesting.